CHALMERS

Chalmers Publication Library

A flexible graphene terahertz detector

This document has been downloaded from Chalmers Publication Library (CPL). It is the author´s version of a work that was accepted for publication in:

Applied Physics Letters (ISSN: 0003-6951)

Citation for the published paper:
Yang, X. ; Vorobiev, A. ; Generalov, A. et al. (2017) "A flexible graphene terahertz detector". Applied Physics Letters, vol. 111(2), pp. 021102-1-021102-4.

http://dx.doi.org/10.1063/1.4993434

Downloaded from: http://publications.lib.chalmers.se/publication/250600

Notice: Changes introduced as a result of publishing processes such as copy-editing and formatting may not be reflected in this document. For a definitive version of this work, please refer to the published source. Please note that access to the published version might require a subscription.

Chalmers Publication Library (CPL) offers the possibility of retrieving research publications produced at Chalmers University of Technology. It covers all types of publications: articles, dissertations, licentiate theses, masters theses, conference papers, reports etc. Since 2006 it is the official tool for Chalmers official publication statistics. To ensure that Chalmers research results are disseminated as widely as possible, an Open Access Policy has been adopted.
The CPL service is administrated and maintained by Chalmers Library.

(article starts on next page)

A flexible graphene terahertz detector

Xinxin Yang, Andrei Vorobiev, Andrey Generalov, Michael A. Andersson, and Jan Stake

Citation: Appl. Phys. Lett. **111**, 021102 (2017); doi: 10.1063/1.4993434
View online: http://dx.doi.org/10.1063/1.4993434
View Table of Contents: http://aip.scitation.org/toc/apl/111/2
Published by the American Institute of Physics

A flexible graphene terahertz detector

Xinxin Yang,[a] Andrei Vorobiev, Andrey Generalov, Michael A. Andersson, and Jan Stake
Department of Microtechnology and Nanoscience, Chalmers University of Technology, SE-41296 Gothenburg, Sweden

(Received 4 May 2017; accepted 28 June 2017; published online 10 July 2017)

We present a flexible terahertz (THz) detector based on a graphene field-effect transistor fabricated on a plastic substrate. At room temperature, this detector reveals voltage responsivity above 2 V/W and estimated noise equivalent power (NEP) below 3 nW/$\sqrt{\text{Hz}}$ at 487 GHz. We have investigated the effects of bending strain on DC characteristics, voltage responsivity, and NEP of the detector, and the results reveal its robust performance. Our findings have shown that graphene is a promising material for the development of THz flexible technology. *© 2017 Author(s). All article content, except where otherwise noted, is licensed under a Creative Commons Attribution (CC BY) license (http://creativecommons.org/licenses/by/4.0/).* [http://dx.doi.org/10.1063/1.4993434]

There is increasing interest for terahertz (THz) technology in various applications, such as information and communications, surveillance and security screening, biomedical and material diagnostics, and global environmental monitoring.[1,2] Over the past few decades, many breakthroughs in high-power sources,[3] room-temperature detectors,[4,5] and real-time imaging[6,7] have pushed the THz research into future novel applications with significant potential, such as wearable smart electronics and multiple transmit and receive antenna systems (MIMO). However, many of these applications call for flexible, portable, and less expensive solutions compared to existing solid-state technologies.

The advancements in polymer technology have promoted flexible electronics and enabled the fabrication of high-frequency devices on flexible substrates for lightweight, low-cost, and shape-conforming applications. In the radio frequency range, flexible sensing/communication devices have been embedded into clothing or other fabrics.[8,9] Thus far, however, only one flexible THz device has been reported: a scanner based on carbon nanotubes.[10] A flexible THz detector can be a key element for future niche applications, for instance, bendable THz electronics for high-speed indoor wireless communication and rf-energy harvesting and wearable THz sensors for medical applications. The quest for a material system and the device concept that allow flexible THz electronics is still a great challenge.

As the first real two-dimensional material, graphene possesses extreme thinness and the ability to reversibly undergo high strains and strain rates.[11,12] With respect to preparation, graphene can be grown over large areas by chemical vapor deposition (CVD) and subsequently transferred to any substrate. Moreover, graphene, which possesses a high intrinsic carrier mobility, high conductivity, and gapless spectrum, has potential for developing detectors,[13,14] sources,[15] and modulators[16] in the THz range.

Here, we report a flexible THz detector based on an antenna-coupled graphene field-effect transistor (GFET) and demonstrate room-temperature THz detection from 330 GHz to 500 GHz. Additionally, the effect of bending strain on the detector performance is also investigated and analyzed.

The detector was fabricated on a flexible and transparent polyethylene terephthalate (PET) substrate with a dielectric constant of 2.6 (see the supplementary material for detail fabrication processes). Figure 1(a) presents images of the detector with a gate length and channel width of 5.5 μm and 4 μm, respectively. The access area gaps between the gate and source/drain are 0.5 μm. The THz power is received by a split bow-tie antenna, which provides an asymmetric coupling condition between the source and drain.[13] The gate capacitance per unit area (C_G) is 6.6 fF/μm^2, as extracted from the S-parameters.

The detector was characterized using the experimental setup shown in Fig. 1(c) (supplementary material). Since the layered structure of the detector is considerably thinner than that of the substrate, the following simple approximation can be used for the tensile strain in the graphene film:[17] $\varepsilon = t/2r$, where t is the thickness of the PET substrate and r is the radius of curvature. The detector was operated in the cold mode, i.e., $V_{ds} = 0$, to minimize $1/f$ noise and maximize sensitivity.[18] The THz voltage responsivity was calculated as

$$R_v = \frac{2\sqrt{2}\Delta U}{P}, \tag{1}$$

where the factor 2 is due to the peak-to-peak amplitude and the factor $\sqrt{2}$ originates from the lock-in amplifier rms amplitude. P and ΔU are the total available THz beam power and the rectified THz voltage of the detector, respectively (see the supplementary material for detail measurements).

Figure 2(a) shows the conductance of the detector versus the gate-source voltage (V_{GS}) with different bending strains of $\varepsilon = 0\%$, 0.875%, and 1.25%. The conductance is calculated as $G = I_{DS}/V_{DS}$, where I_{DS} and V_{DS} are the drain current and the drain-source voltage, respectively, from the transfer characteristics measured at $V_{DS} = 0.5$ mV. As shown in this figure, the Dirac voltages (V_{Dir}) of the detector are located at positive values of V_{GS}, indicating that the graphene channel is p-type. The asymmetric conductance curves are due to the additional resistance produced by the p-n junctions between the n-type gated channel and the p-type ungated regions at

[a]Author to whom correspondence should be addressed: xinxiny@chalmers.se.

 © Author(s) 2017.

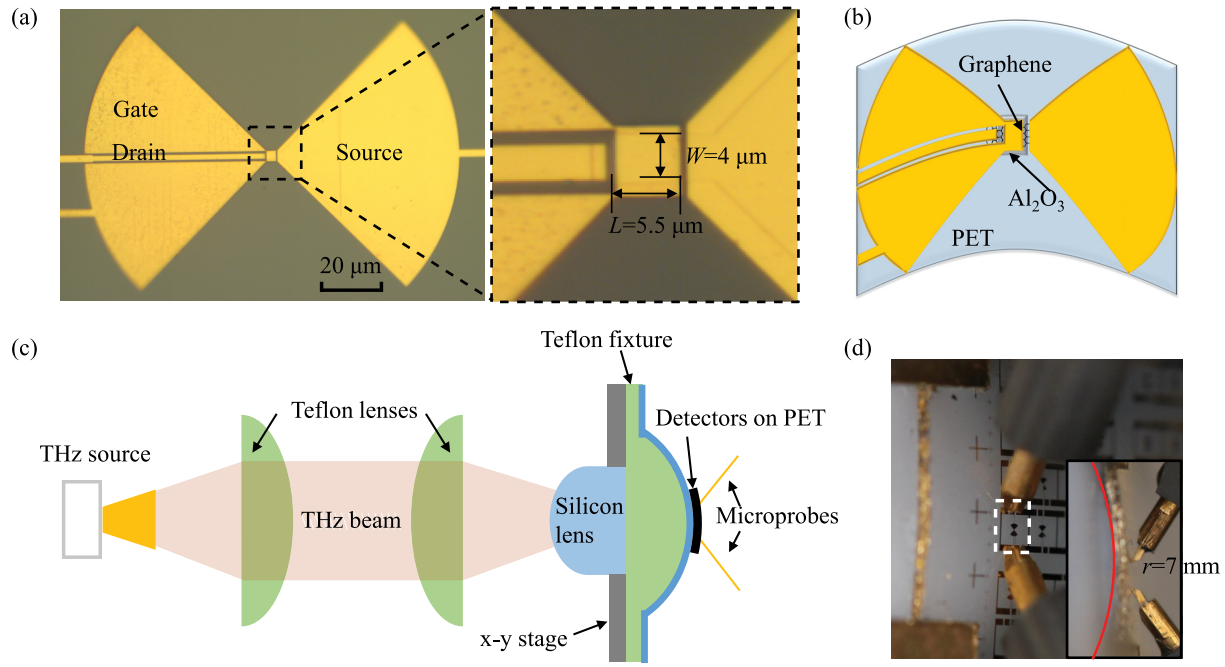

FIG. 1. Flexible GFET-THz detector and experimental setup. (a) Optical microscopy images of the detector. (b) Schematic of the bent detector. (c) Experimental setup for THz characterization. The figure is only for reference, not in the actual size. (d) Photographs of the detector under test with a bending radius of $r = 7$ mm, which corresponds to a strain of $\varepsilon = 1.25\%$. The inset shows the corresponding side view.

positive values of V_{GS}. For the analysis, we assume that graphene transport properties are dominated by Coulomb scattering and that the mobility does not depend on the concentration of the charge carriers.[19] This assumption allows for extraction of the electron/hole mobility ($\mu_{e/h}$) and residual carrier concentration (n_0) by fitting a commonly used semi-empirical model[20] to the measured conductance data in Fig. 2(a). The solid line in Fig. 2(a) represents the fitting results at $\varepsilon = 0\%$. According to our calculations, the average values of μ and n_0 with different strains are $2700\,\mathrm{cm^2/Vs}$ and $1.2 \times 10^{12}\,\mathrm{cm^{-2}}$, respectively, and do not reveal a clear dependence on the strain. The latter can be explained by the fact that the deviations of the mobility with strain in the studied range are less than the uncertainty produced by the fitting model.[21]

As shown in Fig. 2(a), the V_{Dir} of the detector increases with the strain, which is in qualitative agreement with the results presented in Ref. 22 and 23. The shift of the V_{Dir} can be explained by changes in device electrostatics caused by changes in mobile trapped charges in the gate dielectric and

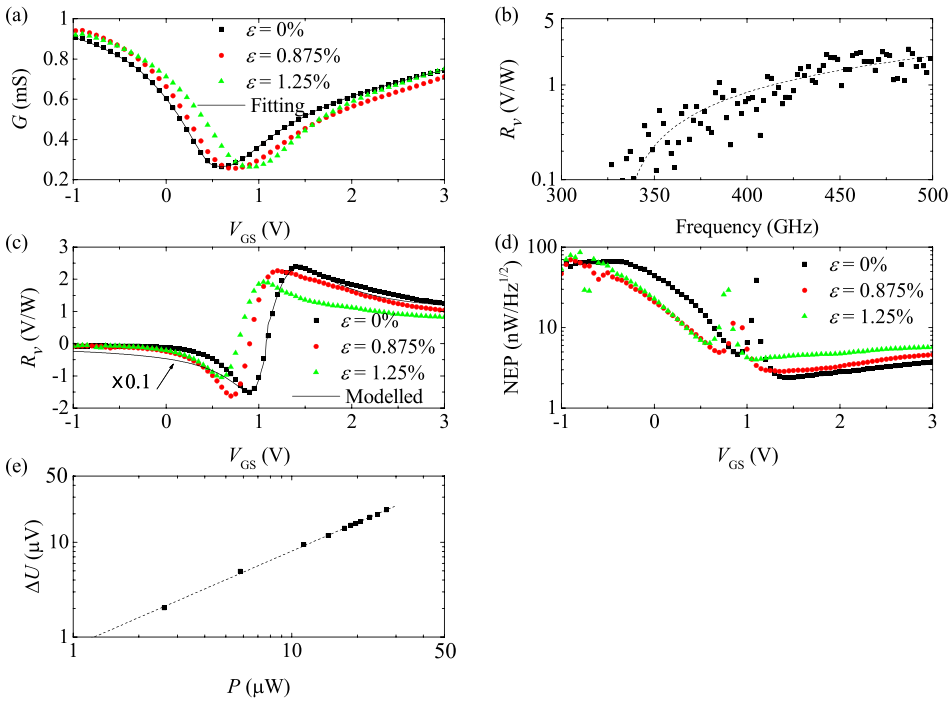

FIG. 2. Detector Characterization. (a) The conductance of the detector as a function of V_{GS} at $V_{DS} = 0.5$ mV with different strains of 0%, 0.875%, and 1.25%. The solid line is the fitting results without strain. (b) The measured R_v as a function of frequency at $V_{GS} = 1.4$ V without strain. The black square markers are the experimental data, and the dashed line is a fit to the data. (c) The measured R_v as a function of V_{GS} at 487 GHz with different strains of 0%, 0.875%, and 1.25%. The solid line is the modelled results without strain. (d) The estimated NEP as a function of V_{GS} at 487 GHz with different strains of 0%, 0.875%, and 1.25%. (e) The measured THz voltage response of the detector as a function of the available THz power at 487 GHz with $V_{GS} = 1.4$ V and without strain.

at the graphene-dielectric interface as the substrate is bending.[23] In particular, it was shown that the stress is responsible for the change in the trap activation energy level.[24]

Figure 2(b) shows the voltage responsivity versus frequency in the entire available frequency range measured at $V_{GS} = 1.4$ V and without bending (the data with strains are shown in the supplementary material). As shown, the voltage responsivity generally increases with the frequency up to approximately 2 V/W. According to our experiments, the deviations around the average value are very reproducible; hence, they can be associated with the standing waves in the optical setup.[25] The increase in the responsivity with frequency can be explained by the increase in the transmitting and detector antenna gains and possibly by better conjugate impedance matching at the higher frequencies.[25–28]

Figure 2(c) shows the measured voltage responsivity as a function of the gate voltage at 487 GHz with different strains. As shown in this figure, the maximum value of the responsivity decreases with the strain. An empirical nonlinear equivalent circuit model predicts a second-order nonlinear response in the GFET-based THz detectors when an oscillating THz field is applied between the gate and source such that[28]

$$R_v \propto \frac{1}{\sigma}\frac{d\sigma}{dV_{GS}}, \tag{2}$$

where σ is the channel conductivity. It can be shown that the both overdamped plasma model and thermoelectric model arrive at a similar V_{GS} dependence.[14,29] The second derivative of the channel conductivity in the form of $\sigma = \sqrt{n_0^2 + (V_{GS}C_G/e)^2}e\mu_{e/h}$ provides the maximum of the responsivity as

$$R_{v,max} \propto \frac{C_G}{2n_0 e}. \tag{3}$$

As shown in Eq. (3), a decrease in the dielectric constants due to the out-of-plane compressive strain caused by bending should result in a decrease in the responsivity. Additionally, in accordance with the model of screening of the charged impurity potential, one can expect an increase in n_0 with a decrease in the dielectric constant because of the reduced screening effect. Indeed, the model provides the following relationship:[30]

$$\frac{n_0}{n_{imp}} = 2r_s^2 C_0, \tag{4}$$

where C_0 is the voltage fluctuation, $r_s = e^2/(k\hbar\nu_F)$ is the effective fine structure constant, ν_F is the Fermi velocity, and k is the dielectric constant. Therefore, the bending strain should result in an increase in n_0 due to the lower dielectric constant and hence a decrease in the voltage response. Thus, the reduction in the voltage response with bending strain observed in our experiments [see Fig. 2(c)] is consistent with the empirical nonlinear model. The solid line in Fig. 2(c) represents the simulation results at $\varepsilon = 0\%$ based on the model. As the gate voltage increases, the measured responsivity varies from negative to positive, which is consistent with the modelled responsivity. However, the amplitude of the modelled responsivity is 10 times larger than that from the measurements since the voltage responsivity calculated using Eq. (1) is underestimated, which does not take into account several other power reduction factors, including the power losses in the experimental setup, limited detector antenna gain, and impedance mismatch between the antenna and transistor.[25–27,31]

The noise equivalent power (NEP) of the detector with zero bias is dominated by thermal Johnson-Nyquist noise and can be calculated as

$$NEP = \frac{\sqrt{4k_B T/G}}{R_v}, \tag{5}$$

where k_B is the Boltzmann constant and $T = 300$ K is the room temperature. Figure 2(d) shows the estimated NEP of the detector as a function of V_{GS} with different strains. The minimum NEP value without bending is less than 3 nW/$\sqrt{\text{Hz}}$ at $V_{GS} = 1.45$ V in the n-type gated channel. As the strain increases from 0% to 1.25%, the minimum NEP increases from 2.4 nW/$\sqrt{\text{Hz}}$ to 4 nW/$\sqrt{\text{Hz}}$, which reflects the excellent mechanical properties of graphene.

Figure 2(e) shows that the measured THz voltage response of the detector at the given $V_{GS} = 1.4$ V is linear with the incident THz power. The available output power from the rf-source was not able to drive the detector into saturation.

In summary, we have presented a flexible THz detector based on an antenna-coupled GFET for the development of novel THz devices. The THz responses of the detector with different strains and different frequencies were measured. The detector without bending offers THz voltage responsivity above 2 V/W and an NEP below 3 nW/$\sqrt{\text{Hz}}$ at 487 GHz for room-temperature operation. Based on the bending tests, the responsivity only has a small reduction with increasing strain, which demonstrates the robustness of the detector. Furthermore, this work provides an important route towards high-performance and low-cost THz flexible technology.

See supplementary material for device fabrication and the experimental setup.

This work was supported in part by the EU Graphene Flagship, in part by the Swedish Foundation of Strategic Research (SSF) under Grant No. SE13-0061, and in part by the Knut and Alice Wallenberg Foundation (KAW). The authors thank Maris Bauer of Johann Wolfgang Goethe-Universität for his help with THz power calibration.

[1]M. Tonouchi, "Cutting-edge terahertz technology," Nat. Photonics **1**, 97–105 (2007).
[2]P. H. Siegel, "Terahertz technology," IEEE Trans. Microwave Theory Tech. **50**, 910–928 (2002).
[3]B. S. Williams, "Terahertz quantum-cascade lasers," Nat. Photonics **1**, 517–525 (2007).
[4]F. Schuster, D. Coquillat, H. Videlier, M. Sakowicz, F. Teppe, L. Dussopt, B. Giffard, T. Skotnicki, and W. Knap, "Broadband terahertz imaging with highly sensitive silicon CMOS detectors," Opt. Express **19**, 7827–7832 (2011).
[5]L. Liu, J. L. Hesler, H. Xu, A. W. Lichtenberger, and R. M. Weikle, "A broadband quasi-optical terahertz detector utilizing a zero bias

Schottky diode," IEEE Microwave Wireless Compon. Lett. **20**, 504–506 (2010).
[6]G. C. Trichopoulos, H. L. Mosbacker, D. Burdette, and K. Sertel, "A broadband focal plane array camera for real-time THz imaging applications," IEEE Trans. Antennas Propag. **61**, 1733–1740 (2013).
[7]C. M. Watts, D. Shrekenhamer, J. Montoya, G. Lipworth, J. Hunt, T. Sleasman, S. Krishna, D. R. Smith, and W. J. Padilla, "Terahertz compressive imaging with metamaterial spatial light modulators," Nat. Photonics **8**, 605–609 (2014).
[8]X. Huang, T. Leng, M. Zhu, X. Zhang, J. Chen, K. Chang, M. Aqeeli, A. K. Geim, K. S. Novoselov, and Z. Hu, "Highly flexible and conductive printed graphene for wireless wearable communications applications," Sci. Rep. **5**, 18298 (2014).
[9]J. Noh, M. Jung, Y. Jung, C. Yeom, M. Pyo, and G. Cho, "Key issues with printed flexible thin film transistors and their application in disposable RF sensors," Proc. IEEE **103**, 554–566 (2015).
[10]D. Suzuki, S. Oda, and Y. Kawano, "A flexible and wearable terahertz scanner," Nat. Photonics **10**, 809–813 (2016).
[11]C. Lee, X. Wei, J. W. Kysar, and J. Hone, "Measurement of the elastic properties and intrinsic strength of monolayer graphene," Science **321**, 385–388 (2008).
[12]M. K. Blees, A. W. Barnard, P. A. Rose, S. P. Roberts, K. L. McGill, P. Y. Huang, A. R. Ruyack, J. W. Kevek, B. Kobrin, D. A. Muller *et al.*, "Graphene kirigami," Nature **524**, 204–207 (2015).
[13]A. Zak, M. A. Andersson, M. Bauer, J. Matukas, A. Lisauskas, H. G. Roskos, and J. Stake, "Antenna-integrated 0.6 THz FET direct detectors based on CVD graphene," Nano Lett. **14**, 5834–5838 (2014).
[14]L. Vicarelli, M. Vitiello, D. Coquillat, A. Lombardo, A. Ferrari, W. Knap, M. Polini, V. Pellegrini, and A. Tredicucci, "Graphene field-effect transistors as room-temperature terahertz detectors," Nat. Mater. **11**, 865–871 (2012).
[15]J. Tong, M. Muthee, S.-Y. Chen, S. K. Yngvesson, and J. Yan, "Antenna enhanced graphene THz emitter and detector," Nano Lett. **15**, 5295–5301 (2015).
[16]B. Sensale-Rodriguez, R. Yan, S. Rafique, M. Zhu, W. Li, X. Liang, D. Gundlach, V. Protasenko, M. M. Kelly, D. Jena *et al.*, "Extraordinary control of terahertz beam reflectance in graphene electro-absorption modulators," Nano Lett. **12**, 4518–4522 (2012).
[17]J. Lewis, "Material challenge for flexible organic devices," Mater. Today **9**, 38–45 (2006).
[18]A. Lisauskas, S. Boppel, J. Matukas, V. Palenskis, L. Minkevičius, G. Valušis, P. Haring- Bolívar, and H. G. Roskos, "Terahertz responsivity and low-frequency noise in biased silicon field-effect transistors," Appl. Phys. Lett. **102**, 153505 (2013).
[19]S. Adam, E. H. Hwang, V. M. Galitski, and S. D. Sarma, "A self-consistent theory for graphene transport," Proc. Natl. Acad. Sci. U. S. A. **104**, 18392–18397 (2007).
[20]S. Kim, J. Nah, I. Jo, D. Shahrjerdi, L. Colombo, Z. Yao, E. Tutuc, and S. K. Banerjee, "Realization of a high mobility dual-gated graphene field-effect transistor with Al_2O_3 dielectric," Appl. Phys. Lett. **94**, 062107 (2009).
[21]X. He, L. Gao, N. Tang, J. Duan, F. Xu, X. Wang, X. Yang, W. Ge, and B. Shen, "Shear strain induced modulation to the transport properties of graphene," Appl. Phys. Lett. **105**, 083108 (2014).
[22]C.-H. Yeh, Y.-W. Lain, Y.-C. Chiu, C.-H. Liao, D. R. Moyano, S. S. Hsu, and P.-W. Chiu, "Gigahertz flexible graphene transistors for microwave integrated circuits," ACS Nano **8**, 7663–7670 (2014).
[23]N. Petrone, I. Meric, J. Hone, and K. L. Shepard, "Graphene field-effect transistors with gigahertz-frequency power gain on flexible substrates," Nano Lett. **13**, 121–125 (2013).
[24]Y. S. Choi, T. Nishida, and S. E. Thompson, "Impact of mechanical stress on direct and trap-assisted gate leakage currents in p-type silicon metal-oxide-semiconductor capacitors," Appl. Phys. Lett. **92**, 173507 (2008).
[25]M. Bauer, A. Rämer, S. Boppel, S. Chevtchenko, A. Lisauskas, W. Heinrich, V. Krozer, and H. G. Roskos, "High-sensitivity wideband THz detectors based on GaN HEMTs with integrated bow-tie antennas," in *2015 10th European Microwave Integrated Circuits Conference*, EuMIC (IEEE, 2015), pp. 1–4.
[26]S. Boppel, A. Lisauskas, M. Mundt, D. Seliuta, L. Minkevicius, I. Kasalynas, G. Valusis, M. Mittendorff, S. Winnerl, V. Krozer *et al.*, "CMOS integrated antenna-coupled field- effect transistors for the detection of radiation from 0.2 to 4.3 THz," IEEE Trans. Microwave Theory **60**, 3834–3843 (2012).
[27]C. A. Balanis, *Antenna Theory: Analysis and Design* (Wiley, New York, 2016).
[28]M. A. Andersson and J. Stake, "An accurate empirical model based on volterra series for FET power detectors," IEEE Trans. Microwave Theory **64**, 1431–1441 (2016).
[29]X. Cai, A. B. Sushkov, R. J. Suess, M. M. Jadidi, G. S. Jenkins, L. O. Nyakiti, R. L. Myers-Ward, S. Li, J. Yan, D. K. Gaskill *et al.*, "Sensitive room-temperature terahertz detection via the photothermoelectric effect in graphene," Nat. Nanotechnol. **9**, 814–819 (2014).
[30]J.-H. Chen, C. Jang, S. Adam, M. Fuhrer, E. Williams, and M. Ishigami, "Charged-impurity scattering in graphene," Nat. Phys. **4**, 377–381 (2008).
[31]H. Sherry, R. Al Hadi, J. Grzyb, E. Öjefors, A. Cathelin, A. Kaiser, and U. R. Pfeiffer, "Lens-integrated THz imaging arrays in 65 nm CMOS technologies," in *2011 IEEE Radio Frequency Integrated Circuits Symposium*, RFIC (IEEE, 2011), pp. 1–4.